Raman scattering by coupled intersubband-Landau-level excitations in quantum-well structures

R. Borroff and R. Merlin

The Harrison M. Randall Laboratory of Physics, The University of Michigan, Ann Arbor, Michigan 48109-1120

J. Pamulapati and P. K. Bhattacharya

Department of Electrical Engineering and Computer Science, The University of Michigan, Ann Arbor, Michigan 48109-2122

C. Tejedor

Departamento de Física de la Materia Condensada, Universidad Autónoma de Madrid, Cantoblanco, 28049 Madrid, Spain

We report a Raman-scattering investigation of coupled intersubband-Landau-level excitations in GaAs quantum-well structures. Coupling was induced by tilting the magnetic field away from the superlattice axis. The samples were nominally undoped. Carriers at low concentrations ($< 10^9$ cm^{-2}) were generated by means of photoexcitation. Data on various transitions at small tilt angles show very good agreement with results of perturbation theory and, at large angles, with calculations using a finite-basis approximation. Gaps in the excitation spectrum and signatures of the related persisting mixing of levels have been clearly observed. The lowest-lying coupled modes exhibit scaling behavior, following extremely well predictions of the parabolic-well model.

I. INTRODUCTION

Quasi-two-dimensional electron systems in a magnetic field generally exhibit coupling between the (originally independent) motions parallel and perpendicular to the confinement plane.[1-24] The tilt angle θ, defined by the direction of the field and the normal to the plane, determines the degree of admixture vanishing at $\theta=0$. For various reasons, the spectrum of confined electrons in tilted fields has been the object of intensive study in recent years.[9-24] In the case of free electrons, tilting results in subband-Landau-level hybridization and associated excitations of mixed character.[1-4,6-7,9-22] Experimentally, tilted-field-induced coupling with allowed excitations makes possible for infrared[9-19] and Raman[21,22] spectroscopy to probe nominally forbidden intersubband or cyclotron resonances. Tilted magnetic fields have also been applied to related studies of confined shallow impurities[21-23] and, more recently, they have helped elucidate the role of reversed spins in the fractional quantum Hall effect.[24]

In this work, we report on a Raman-scattering study of intersubband-Landau-level coupling in quantum-well structures. Our approach distinguishes itself from previous investigations, particularly those dealing with infrared spectroscopy of space-charge layers,[9-17] in several respects. We note first that the confinement potential in quantum wells is *a priori* well defined and, in some sense, robust as opposed to that of space-charge layers depending strongly on doping and boundary conditions. Because a precise determination of the latter is difficult, the comparison between space-charge-layer experiments and theory carries a large degree of uncertainty. For the most part, this problem has been eliminated in our work. Concerning the experimental techniques, there are also some important differences. Raman scattering presents the advantage over infrared spectroscopy of being able to discriminate between spin- and charge-density excitations. Thus, corrections accounting for depolarization-field effects become, to some extent, experimentally accessible. In our studies, we made use of this feature of the scattering only indirectly. To minimize many-body (Hartree) corrections to the potential and various sources of broadening, our measurements were performed at relatively low electron concentrations ($< 10^9$ cm^{-2}) leading to nearly identical spin- and charge-density spectra. The method we employed to achieve such low densities was photoexcitation. Unlike modulation doping, this way of generating carriers minimally alters the shape of the potential because of the evident charge neutrality of the photoexcited electron-hole system. Finally, we probed the spectrum of excitations at energies that are much smaller than the band-gap discontinuities. This was done to avoid a possible source of uncertainty for, in this range, the spectra are rather insensitive to the depth of the confinement potential as the wells behave as infinitely deep.

Other than experiments, we present in this paper results of finite-basis calculations of the tilted-field spectrum and derive selection rules for the coupling relying on the even symmetry of the confinement potential. The calculations and the Raman measurements agree substantially over a broad range of angles and fields. In addition, the finite-basis (and the experimental) data for the *lowest-lying* coupled levels show a remarkable agreement with predictions of the parabolic-potential model.[4,6] This is obviously relevant to recent infrared work on coupled excitations in parabolic wells.[18,19]

II. THEORY

Coupled intersubband-Landau-level excitations have been extensively discussed in the theoretical literature,[1-7]

particularly for quasi-two-dimensional systems which form at metal-semiconductor-oxide structures and semiconductor heterojunctions.[1-3] In this section, we briefly review the main features of the tilted-magnetic-field problem focusing on quantum wells. Within the conventional formalism,[1-3] the differences between the latter and the cases of inversion and accumulation layers represent but a minor point. Although the confinement potential of a quantum well leads to a somehow more tractable situation because it is of even symmetry and, for our purposes, independent of carrier density (as opposed to the triangularlike potential of many-body origin in space-charge layers),[1-3] one still needs to deal with a nonseparable Hamiltonian. Nevertheless, there is a distinctive aspect which separates the case of quantum wells. As mentioned previously, their lowest-lying coupled states are well accounted for by the analytically soluble parabolic-potential model.[4,6] This, in a sense, fortuitous circumstance relies mainly on two facts. First, the ground and first excited eigenfunctions of parabolic and square wells are very similar and, next, the hybrid modes in quantum wells couple only weakly to higher-lying states within some range. It is clear that these conditions do not necessarily require a piecewise-constant potential, i.e., parabolic-well solutions certainly apply to other confinement potentials as well.

The Hamiltonian for noninteracting electrons confined in the (x,y) plane and magnetic field $\mathbf{B} = B(0, \sin\theta, \cos\theta)$ can be written as[1-7]

$$H = H_W + H_P + H_D + H_M \ , \tag{1}$$

with

$$H_W = \frac{1}{2m_0}p_z^2 + V(z) \ , \tag{2}$$

$$H_P = \frac{1}{2m_0}p_x^2 + \frac{1}{2m_0}(p_y + \hbar\cos\theta\, x/l^2)^2 \ , \tag{3}$$

and

$$H_D = \frac{\hbar^2}{2m_0}(z^2\sin^2\theta/l^4) \ , \tag{4}$$

$$H_M = (\hbar/m_0)(zp_x\sin\theta/l^2) \ . \tag{5}$$

Here, $\mathbf{p} = (p_x, p_y, p_z)$ and m_0 are the momentum and the effective mass of the electron, θ is the tilt angle, and $l = (c\hbar/eB)^{1/2}$ is the magnetic length. $V(z)$ is the confinement potential; for a quantum well of width L and barrier energy V_0, it is given by

$$V(z) = \begin{cases} V_0 & \text{for } |z| > L/2 \ , \\ 0 & \text{for } |z| \le L/2 \ . \end{cases} \tag{6}$$

The eigenenergies and wave functions of H cannot be obtained analytically. Various methods giving approximate solutions which are adequate for some range of parameters are discussed in the following.

A. Perturbation theory

At $\theta = 0$, $H_D \equiv H_M \equiv 0$ and the motions along z and in the (x,y) plane (determined by H_W and H_P, respectively)

trivially decouple. The eigenstates of H are of the form

$$\psi_{n,N,X}^{(0)}(x,y,z) = \phi_n^{(0)}(z)\chi_{N,X}(x,y) \ , \tag{7}$$

where $\phi_n^{(0)}(z)$ ($n = 0, 1, \ldots$) is the nth eigenstate of H_W and $\chi_{N,X}$ is a Landau state of energy $(N + \frac{1}{2})\hbar\omega_c$ ($N = 0, 1, \ldots$); $\omega_c = eB/m_0c$ is the cyclotron frequency and X is the center coordinate. If θ is small, H_D and H_M can be treated as perturbations.[1-3,6] To lowest order in θ, i.e., first order in H_D and second order in H_M, both terms lead to shifts of the energy levels proportional to $\sin^2\theta$. For $B \to 0$, the H_M contribution behaves as B^3, while that of the diamagnetic term, H_D, is proportional to B^2 and, therefore, dominant. Accordingly, if $\hbar\omega_c$ is negligible compared with intersubband spacings, perturbation theory predicts a B^2-like increase for the eigenenergies (positive diamagnetic shift).[1-3] Moreover, transition energies are also expected to increase with field given that higher-lying wave functions generally show a larger spread, i.e., larger $\langle z^2 \rangle$. Note, however, that the shifts can have either sign if the contribution of the mixing term H_M becomes important (see the example later).[6] H_M couples states with Landau indices differing by ± 1 and is primarily responsible for the crossing-avoiding behavior of levels at points of degeneracies.[1-3]

B. Finite-basis approximation

To compute the electronic states at arbitrary tilt angle, we have applied the formalism developed by Ando.[2] Here, H is represented in the basis

$$\psi_{n,N,X}(x,y,z) = \phi_n(z)\chi_{N,X}(x,y) \ , \tag{8}$$

where

$$(H_W + H_D)\phi_n = \varepsilon_n\phi_n \ . \tag{9}$$

From the eigenstates ϕ_n computed numerically, it is straightforward to calculate the matrix elements of H_M given by[2,3]

$$\langle nN|H_M|n'N'\rangle = (1 - \delta_{n,n'})\frac{\hbar^2 z_{nn'}}{m_0 l^3}\sin\theta\cos^{1/2}\theta$$
$$\times \left[\left[\frac{N'+1}{2}\right]^{1/2}\delta_{N,N'+1} \right.$$
$$\left. + \left[\frac{N'}{2}\right]^{1/2}\delta_{N,N'-1} \right] \tag{10}$$

with $z_{nn'} = \langle \phi_n|z|\phi_{n'}\rangle$. In this expression, we have dropped the center coordinate X, which remains as a good quantum number because H does not depend on y. Since $z_{nn'}$ vanishes unless $(-1)^n \ne (-1)^{n'}$ and the off-diagonal elements are nonzero only for $N = N' \pm 1$, the matrix H_M separates into two blocks corresponding to states with either $(-1)^{n+N} = 1$ or $(-1)^{n+N} = -1$. It follows then that states having $(-1)^{n+N} \ne (-1)^{n'+N'}$ can cross, while no crossing is allowed for $(-1)^{n+N} = (-1)^{n'+N'}$. For simplicity, levels belonging to the $(-1)^{n+N} = \pm 1$ manifolds will be referred to as even $(+)$ and odd $(-)$. In our calculations, we have in-

cluded the states with $n = 0, 1, 2$ and $N = 0, 1, 2, 3, 4, 5$, truncating H_M to a 9×9 matrix.

C. Parabolic-well model

For $V(z) = m_0 \Omega^2 z^2 / 2$, Schrödinger's equation can be solved analytically for arbitrary θ.[4,6] The eigenvalues are of the form $(n_\alpha + \frac{1}{2})\varepsilon_\alpha + (n_\beta + \frac{1}{2})\varepsilon_\beta$, where n_α and n_β are integers and $\varepsilon_\alpha, \varepsilon_\beta$ can be shown to satisfy the relations

$$\varepsilon_\alpha^2 + \varepsilon_\beta^2 = (\hbar\Omega)^2 + (\hbar\omega_c)^2 ,$$
$$\varepsilon_\alpha \varepsilon_\beta = \hbar^2 \omega_c \Omega \cos\theta ,$$

(11)

which are appropriate for scaling purposes. In the comparison with our experiments, we have taken $\Omega = E_{01}\hbar^{-1}$ with the intersubband energy $E_{01} = \varepsilon_1^{(0)} - \varepsilon_0^{(0)}$. Here, $\varepsilon_{0,1}^{(0)}$ are the eigenenergies of the ground and first excited state of H_W or, alternatively, $\varepsilon_{0,1}$ [Eq. (9)] at $\theta = 0$. A few features of these solutions should be emphasized. First, the lower branch of the coupled modes tends to $E_{01}\cos\theta$ at large fields, giving rise to a gap in the excitation spectrum.[6,14,22] This resembles, in some sense, the coupling between photons and infrared-active phonons (polaritons) leading to splitting into transverse and longitudinal modes.[25] In addition, the asymptote of the upper branch is $\hbar\omega_c$, indicating that B (as opposed to $B \cos\theta$) determines the position of the cyclotron resonance for $\hbar\omega_c \gg E_{01}$. However, the lower branch is $\cong \hbar\omega_c \cos\theta$ for $\hbar\omega_c \ll E_{01}$.[6]

III. SAMPLES AND EXPERIMENTAL PROCEDURES

The samples were GaAs-Al$_{1-x}$Ga$_x$As multiple quantum wells grown by molecular-beam epitaxy on (001) semi-insulating GaAs substrates. Three structures with GaAs-well thicknesses $L = 700$ Å (250 Å, $x = 0.3$, 10 periods), 460 Å (125 Å, $x = 0.22$, 20 periods), and 380 Å (200 Å, $x = 0.25$, 50 periods) were studied in detail (the corresponding widths of the Al$_{1-x}$Ga$_x$As barriers, the Al concentration, and the number of periods are given in parentheses); values of E_{01} measured at zero field were 30, 65, and 80 cm^{-1}, respectively. These energies should be compared with $\hbar\omega_c \approx 100$ cm^{-1} for GaAs at $B = 7$ T, the latter being the largest field provided by our split-coil superconducting magnet.

Raman measurements were performed at $T = 4$ K using a DCM (4-dicyanomethylene-2-dimethylaminostyril-4H-pyran) dye laser pumped by an argon-ion laser. The photoelectrons were generated using the same beam. The DCM dye covers the region of the resonance with the critical point derived from the spin-orbit split-off gap of GaAs where electron (although not hole) scattering is enhanced.[26] Power densities were kept purposely low, in the range 0.5–2 W cm^{-2}, to create as small a population as possible (see below) and to avoid thermal broadening. However, some increase in temperature could not be prevented. Measurements of Stokes to anti-Stokes ratios give electronic temperatures in the range 20–35 K. Spectra with a resolution of ≈ 1 cm^{-1} were obtained in the $z(x',y')\bar{z}$ and $z(x',x')\bar{z}$ scattering configurations, where, as before, z is normal to the layers and x',y' are along the

[110] and [1$\bar{1}$0] directions. These geometries allow, respectively, scattering by spin-density and charge-density excitations.[26] It is well known that the carrier concentration can be gained from the positions of intersubband peaks in the two geometries (there is a depolarization shift for the charge-density, but not the spin-density scattering).[26] In our experiments, the power density was reduced to the above-quoted values so that the Raman shifts in $z(x',y')\bar{z}$ and $z(x',x')\bar{z}$ could not be distinguished. From the limiting spectral resolution, we estimate an upper bound of 10^9 cm^{-2} for the photoexcited electron density. At this level, many-body corrections are negligible and, thus, our measurements give essentially the bare transition energies. Moreover, our low-density data show no evidence of broadening due to impurity-related processes (leading to nonvertical transitions), as is commonly observed at much higher carrier concentrations.[27]

IV. RESULTS AND DISCUSSION

Figure 1 shows typical Raman data for the sample with $L = 700$ Å (θ is given in radians). The low-energy peaks labeled by arrows are hybrid excitations involving predominantly the states $|n, N\rangle = |1, 0\rangle$ and $|0, 1\rangle$. In the top trace ($B = 2.15$ T, $\theta = 0.14$), the feature at ≈ 80
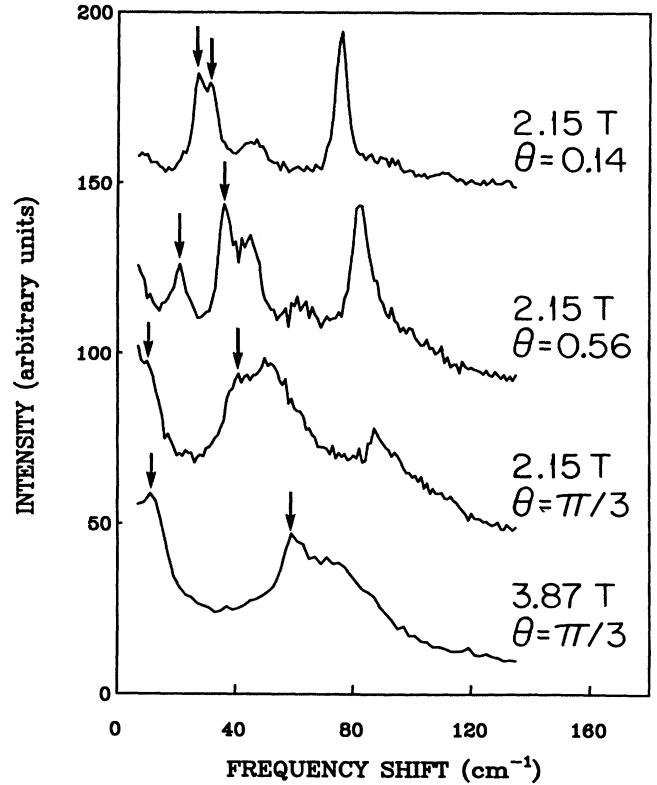
FIG. 1. Electronic $z(x',y')\bar{z}$ Raman spectra of the $L = 700$ Å quantum well at various tilt angles (θ) and magnetic fields. Arrows denote transitions into coupled modes $|0,1\rangle$ and $|1,0\rangle$ (combined intersubband-cyclotron resonances). The temperature is $T = 3.5$ K and the laser energy is 1.873 eV.

cm^{-1} corresponds primarily to the transition $|0,0\rangle \rightarrow |2,0\rangle$, while that at ≈ 45 cm^{-1} is $|1,0\rangle \rightarrow |2,0\rangle$. Data for the same sample at a small tilt angle ($\theta = 0.14$) are shown in Fig. 2. The measurements illustrate crossing avoidances that can be accounted for by perturbation theory. Such a behavior is clearly observed in the spectra for $B = 2.15$–2.5 T (at a shift of ≈ 30 cm^{-1}) and for $B = 3.44$–3.9 T (at ≈ 75 cm^{-1}). The former results from the mixing of the odd states $|1,0\rangle$ and $|0,1\rangle$ and the latter from the even levels $|2,0\rangle$ and $|1,1\rangle$. In both cases, the transitions originate in the ground state $|0,0\rangle$. One should notice that the cyclotron mode, namely the $|0,0\rangle \rightarrow |0,1\rangle$ transition as well as the $|0,0\rangle \rightarrow |1,1\rangle$ excitation, can only be observed when their energies are close to those of intersubband excitations, i.e., in the strong-mixing region. This is not unexpected for transitions with $\Delta N = 1$ are Raman forbidden and, therefore, hybridization with Raman-active modes is a necessary condition for their observation (this contrasts with the usual situation encountered in infrared spectroscopy, where tilted fields lead to absorption by the nominally forbidden intersubband transition). In this regard, we notice that, in

principle, $|0,0\rangle \rightarrow |0,1\rangle$ is not Raman allowed because the states have different parities (this does not apply, of course, to $|0,0\rangle \rightarrow |0,2\rangle$). However, there is evidence[26] indicating that the scattering arises from wave-vector-dependent terms not included in the derivation of the conventional selection rules (for our backscattering geometry, such terms do not permit $\Delta N = 1$ scattering). We also note that our findings differ from those of experiments on modulation-doped structures (high electron densities) where forbidden Raman scattering by the cyclotron mode is observed at $\theta = 0$.[28]

The results in Fig. 2 reveal also signs of other aspects of the intersubband-Landau-level mixing which become more pronounced at large tilt angles. For instance, the data in the range ≤ 60 cm^{-1} suggest a mixing asymmetry in that the intensity of the cyclotron peak is significantly larger after (as opposed to before) the avoided crossing. Similar behavior, more evident in the spectra at $\theta = \pi/3$ in Fig. 1, was observed at various angles in all three sam-

FIG. 2. Magnetic field dependence of the Raman spectra for the sample with $L = 700$ Å at $\theta = 0.14$. The coupled $|0,1\rangle$ and $|1,0\rangle$ modes are indicated by arrows. Dashed lines denote excitations not involving the ground state. The laser energy is 1.873 eV and $T = 3.5$ K. The scattering configuration corresponds to spin-density excitations.
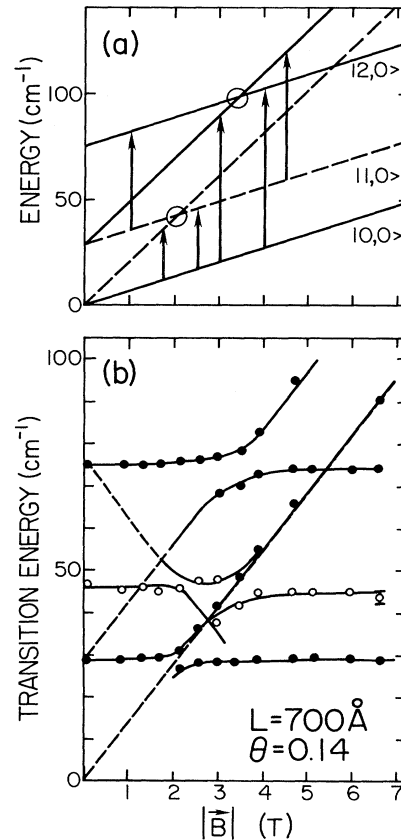
FIG. 3. (a) Dependence of eigenenergies on magnetic field for $L = 700$ Å and $\theta = 0$. Solid (dashed) lines correspond to even- (odd-) parity levels. Circles at crossings denote expected tilt-induced couplings. Transitions identified in the spectra are indicated by arrows. (b) Measured transition energies as a function of B. The solid and open circles are for excitations where the initial state is the ground state and (primarily) the $|1,0\rangle$ level, respectively. The solid lines are guides for the eye. Dashed lines have a slope determined by the effective mass of bulk GaAs.

ples. Moreover, the positions of the intersubband lines $|0,0\rangle \rightarrow |0,1\rangle, |0,2\rangle$ exhibit a small *negative* shift of $\approx 1-2$ cm^{-1} at high fields reflecting the existence of a gap[6,14,22] in the excitation spectrum (as shown later, the shift increases with increasing angle). Both such observations are closely related and consistent with the theoretical results; gaps obviously require that the coupled modes remain mixed long after their energies cross. The calculations using the finite-basis approximation and the parabolic-well model[4,6] show indeed the occurrence of gaps and persistent mixing as $B \rightarrow \infty$. Their origin can be traced back to the fact that the mixing term H_M is not a constant, but a function of B. Interestingly, the theory also indicates that the energies of the upper branches are not affected by the hybridization.[6] This establishes an additional link with the (photon-phonon) polariton problem.[25]

The plots in Fig. 3 summarize the results for the $L = 700$ Å structure at $\theta = 0.14$ and their analysis. Fig-

ure 3(a) depicts the energies of the relevant *uncoupled* levels as a function of magnetic field. Because θ is small, mixing is only important in the immediate vicinity of the degeneracies indicated by the two circles. The measured transition energies are shown in Fig. 3(b). Here, there are a few data points associated with transitions into essentially pure states with $N = 1$, i.e., $|0,0\rangle \rightarrow |0,1\rangle, |1,1\rangle$, which can be used to determine the effective mass (the data follow a linear dependence with the field, as shown by the dashed lines). From the slopes, we find $m_0/m_E = 0.068 \pm 0.002$, to be compared with $m_0/m_E = 0.0665$ for bulk GaAs (m_E is the electron mass).[29] Our experimental values are consistent with perturbation theory in regard to the magnitude of the diamagnetic shifts and the avoidances.[1-3] In particular, the measured distances for the closest approach of coupled modes $\{|0,1\rangle, |1,0\rangle\}$ and $\{|1,1\rangle, |0,2\rangle\}$ agree within 5% with theoretical predictions. Unfortunately, the diamagnetic shifts outside the mixing regions are too small to provide a meaningful comparison with theory.

Data at a large angle ($\theta = \pi/3$) for the three samples are shown in Fig. 4. The most significant feature of these results is the anticipated large gap separating the lowest $\{|0,1\rangle, |1,0\rangle\}$ hybrid excitations [the lowest two branches in Fig. 4(b)]. In the range of interest, the spectrum of our quantum wells is well approximated by that of an infinitely deep potential and, at a fixed angle, the latter can be scaled for arbitrary L if one chooses E_{01} [$\approx 3\pi^2 \hbar^2/(2m_0 L^2)$] as the unit of energy. The calculations in Fig. 4 using the finite-basis approximation are for $V_0 = \infty$ [Eq. (6)]. Theory and experiment agree extremely well other than for the second branch from the top. The source of this discrepancy has not been identified as yet. The branch corresponds to the transition into a level resulting from the hybridization of mainly three states: $|0,2\rangle, |2,0\rangle$, and $|1,1\rangle$.

For $\hbar\omega_c \geq E_{01}$, finite-basis calculations at large angles
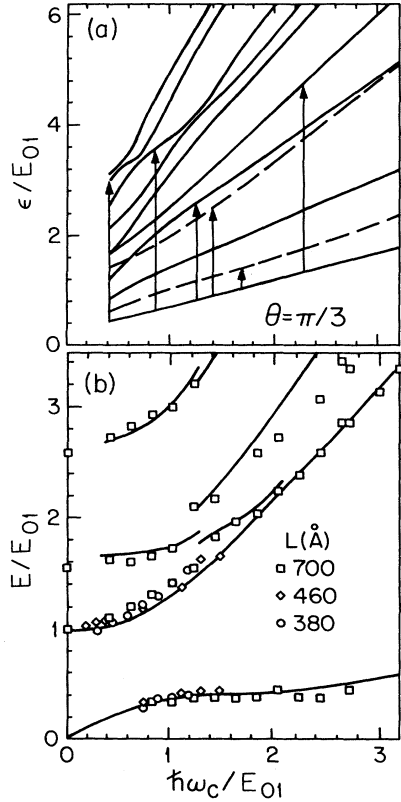
FIG. 4. (a) Energy levels of an infinitely deep quantum well (arbitrary L) at $\theta = \pi/3$ as a function of cyclotron energy ($\hbar\omega_c$) calculated using the finite-basis approximation discussed in the text. The scales are normalized to the energy separation between the two lowest quantum-well states at zero field, E_{01}. Solid (dashed) curves indicate even- (odd-) parity levels. Arrows denote transitions from the ground state observed in the experiments. (b) Comparison between calculated and measured transition energies ($\theta = \pi/3$). The second branch from the top at $\hbar\omega_c = 0$ is the intersubband excitation $|1,0\rangle \rightarrow |2,0\rangle$. Other branches correspond to the transitions labeled by arrows in (a).
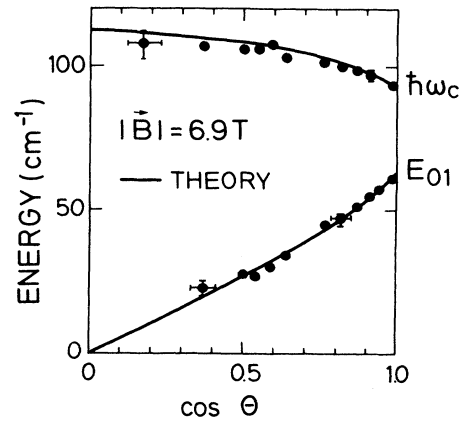
FIG. 5. Angular dependence of the energies of the coupled intersubband-cyclotron modes ($|0,1\rangle$ and $|1,0\rangle$) at $B = 6.9$ T for the sample with $L = 460$ Å. Experimental data (dots) were obtained at $T = 4.1$ K and a laser energy of 1.921 eV. Theoretical results are for the parabolic-well model.
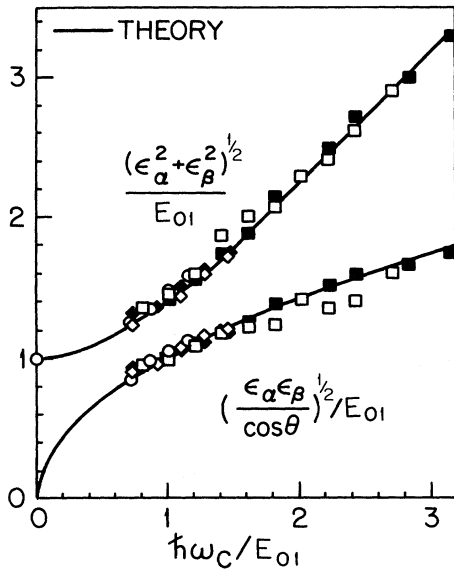
FIG. 6. Scaled plot of experimental data for three samples (squares, 700 Å; diamonds, 460 Å; circles, 380 Å) at two different angles. ϵ_α and ϵ_β denote the energies of the coupled intersubband-cyclotron modes ($|0,1\rangle$ and $|1,0\rangle$). Solid (open) symbols are for $\theta = 0.14$ ($\theta = \pi/3$). $\hbar\omega_c$ is the cyclotron energy and E_{01} is the intersubband energy associated with the two lowest states of the well at zero field. The solid lines are results of the parabolic-well model [Eq. (11)].

show (in most cases) strong mixing involving a large number of states with comparable weights. However, the lowest two branches contain nearly exclusively a combination of $|0,1\rangle$ and $|1,0\rangle$. This, and the mentioned fact that $|0,0\rangle$ and $|1,0\rangle$ in parabolic and square wells are very similar,[21,22] provide a justification for the applicability of the parabolic-potential model to our problem. Actually, finite-basis and parabolic-well results[4,6] for the lowest two branches exhibit substantial agreement over a wide range of angles and fields. As shown in Figs. 5 and 6, our measurements also agree remarkably well with

parabolic-potential predictions. Figure 5 illustrates the dependence of the coupled-mode frequencies on θ for a value of the field at which $\hbar\omega_c > E_{01}$. The data, for the sample with $L = 460$ Å, reveal a *negative* shift of the intersubband peak with increasing angle, reflecting the dominance of H_M over H_D.[6] Also note that, as expected, the energy of the lower branch approaches zero as $\theta \to \pi/2$. Finally, the results in Fig. 6 for the three samples and two different angles closely follow the scaled expressions [Eq. (11)] valid for parabolic wells. We remark that, *a priori*, there are no reasons for piecewise-constant potentials (including $V_0 = \infty$) to exhibit such scaling form.

V. CONCLUSIONS

Hybrid intersubband-Landau-level excitations of photoexcited electrons in quantum-well structures have been studied using resonant Raman scattering for a wide range of tilt angles and fields. The results were obtained at very low power (electron) densities to minimize broadening effects. Various transitions associated with mainly the states $|n,N\rangle = |0,0\rangle$, $|1,0\rangle$, $|2,0\rangle$, $|0,1\rangle$, and $|1,1\rangle$ were identified (n and N label, respectively, the subbands and the Landau levels). The measurements show very good agreement with (single-particle) finite-basis calculations involving no free parameters. The existence of gaps in the excitation spectrum as well as the persistence of mixing far beyond degeneracies have been clearly demonstrated. It has also been shown that the parabolic-potential model accurately describes the behavior of the lowest-lying coupled modes $|1,0\rangle$ and $|0,1\rangle$ and, in particular, that their eigenenergies closely follow a scaling law valid for parabolic wells.

ACKNOWLEDGMENTS

[1]F. Stern and W. E. Howard, Phys. Rev. **163**, 816 (1967).

[2]T. Ando, Phys. Rev. B **19**, 2106 (1979).

[3]T. Ando, A. B. Fowler, and F. Stern, Rev. Mod. Phys. **54**, 437 (1982).

[4]J. C. Maan, in *Two Dimensional Systems, Heterostructures, and Superlattices*, edited by G. Bauer, F. Kuchar, and H. Heinrich (Springer, Berlin, 1984), p. 183.

[5]B. Huckestein and R. Kümmel, Z. Phys. B **66**, 475 (1987).

[6]R. Merlin, Solid State Commun. **64**, 99 (1987).

[7]M. Za*l*uzny, Phys. Rev. B **40**, 8495 (1989).

[8]D. C. Tsui, Solid State Commun. **9**, 1789 (1971).

[9]W. Beinvogl and J. F. Koch, Phys. Rev. Lett. **40**, 1736 (1978).

[10]Z. Schlesinger, J. C. M. Hwang, and S. J. Allen, Jr., Phys. Rev. Lett. **50**, 2098 (1983).

[11]G. L. J. A. Rikken, H. Sigg, C. J. G. M. Langerak, H. W. Myron, J. A. A. J. Perenboom, and G. Weimann, Phys. Rev. B **34**, 5590 (1986).

[12]M. A. Brummell, M. A. Hopkins, R. J. Nicholas, J. C. Portal, K. Y. Cheng, and A. Y. Cho, J. Phys. C **19**, L107 (1986).

[13]A. D. Wieck, J. C. Maan, U. Merkt, J. P. Kotthaus, K. Ploog, and G. Weimann, Phys. Rev. B **35**, 4145 (1987).

[14]S. Huant, M. Grynberg, G. Martinez, and B. Etienne, Solid State Commun. **65**, 457 (1988).

[15]A. D. Wieck, F. Thiele, U. Merkt, K. Ploog, G. Weimann, and W. Schlapp, Phys. Rev. B **39**, 3785 (1989).

[16]K. Ensslin, D. Heitmann, and K. Ploog, Phys. Rev. B **39**, 10 879 (1989).

[17]S. Huant, G. Martinez, and B. Etienne, Superlatt. Microstruct. **6**, 103 (1989).

[18]M. Shayegan, T. Sajoto, J. Jo, M. Santos, and H. D. Drew, Phys. Rev. B **40**, 3476 (1989).

[19]K. Karrai, H. D. Drew, M. W. Lee, and M. Shayegan, Phys. Rev. B **39**, 1426 (1989).

[20]V. E. Kirpichev, I. V. Kukushkin, V. B. Timofeev, and V. I.

Fal'ko, Zh. Eksp. Teor. Fiz. **51**, 383 (1990) [JETP Lett. **51**, 436 (1990)]; J. J. Koning et al., Phys. Rev. B **42**, 2951 (1990).

[21] R. Borroff, R. Merlin, R. L. Greene, and J. Comas, Superlatt. Microstruct. **3**, 493 (1987).

[22] R. Borroff, R. Merlin, R. L. Greene, and J. Comas, Surf. Sci. **196**, 626 (1988).

[23] N. C. Jarosic, E. Castano, B. D. McCombe, Y. C. Lee, J. Ralston, and G. Wicks, Surf. Sci. **170**, 459 (1986).

[24] R. G. Clark, S. R. Haynes, A. M. Suckling, J. R. Mallett, P. A. Wright, J. J. Harris, and C. T. Foxon, Phys. Rev. Lett. **62**, 1536 (1989); J. P. Eisenstein, H. L. Störmer, L. Pfeiffer, and K. W. West, ibid. **62**, 1540 (1989); V. Halonen, P. Pietiläinen, and T. Chakraborty, Phys. Rev. B **41**, 10 202 (1990).

[25] M. Born and K. Huang, Dynamical Theory of Crystal Lattices (Clarendon, Oxford, 1954).

[26] See, e.g., G. Abstreiter and A. Pinczuk, in Light Scattering in Solids V, Vol. 66 of Topics in Applied Physics, edited by M. Cardona and G. Güntherodt (Springer, Berlin, 1989), p. 153.

[27] A. Pinczuk, J. M. Worlock, H. L. Störmer, A. C. Gossard, and W. Wiegmann, J. Vac. Sci. Technol. **19**, 561 (1981).

[28] J. M. Worlock, A. Pinczuk, Z. J. Tien, C. H. Perry, H. Störmer, R. Dingle, A. C. Gossard, W. Wiegmann, and R. L. Aggarwal, Solid State Commun. **40**, 867 (1981); A. Pinczuk, D. Heiman, A. C. Gossard, and J. H. English, in Proceedings of the 18th International Conference on the Physics of Semiconductors, edited by O. Engström (World Scientific, Singapore, 1987), p. 557.

[29] Q. H. F. Vrehen, J. Phys. Chem. Solids **29**, 129 (1968).